Pergamon

Ultrasound in Med. & Biol., Vol. 20, No. 1, pp. 53–63, 1994

0301-5629/94 $6.00 + .00

0301-5629(94)E0004-V

●*Original Contribution*

EFFECTS OF PULSED ULTRASOUND ON THE MOUSE NEONATE: HIND LIMB PARALYSIS AND LUNG HEMORRHAGE

LEON A. FRIZZELL, ELLEN CHEN[†] and CHONG LEE[‡]

Bioacoustics Research Laboratory, Department of Electrical and Computer Engineering, University of Illinois, 1406 W. Green Street, Urbana, IL 61801, USA

(*Received* 1 *September* 1992; *in final form* 2 *June* 1993)

Abstract—Exposure conditions were determined for hind limb paralysis and lung hemorrhage of neonatal mice due to pulsed exposure (10 μs pulse duration) to 1 MHz focused ultrasound. Spatial peak pulse average intensity and peak rarefactional pressure levels for paralysis in 50% of specimens sonicated were determined for pulse repetition frequencies of 1, 5 and 50 kHz at 10°C and 2.4 s exposure duration. The results suggest that cavitation was involved in the paralysis at a pulse repetition frequency (PRF) of 50 kHz, but that cavitation took place in the coupling medium and probably not within the specimen during exposures at a PRF of 5 kHz. The results show an inverse relation between spatial peak pulse average intensity, or peak rarefactional pressure and sound on-time. Exposure conditions for lung hemorrhage were determined for a pulse duration of 10 μs at 10°C and exposure durations of 2.4 and 180 s. The results show that the threshold exposure conditions for lung hemorrhage are much less than the conditions for cavitational or other effects reported for tissues that do not contain well defined gas bodies. In addition, the results show an inverse relation between exposure level and either exposure duration or sound on-time, suggesting that time is an important parameter associated with bubble effects.

Key Words: **Ultrasound, Bioeffects, Mouse neonates, Hind limb paralysis, Lung, Hemorrhage, Cavitation, Pulsed.**

INTRODUCTION

In recent years the potential for biological effects associated with clinical ultrasound has become of increasing concern. This is, in part, a result of theoretical predictions (Apfel 1982, 1986; Flynn 1982; Carstensen and Flynn 1982; Holland and Apfel 1989) and experimental measurements (Crum and Fowlkes 1986; Fowlkes and Crum 1988; Atchley et al. 1988) of transient cavitation occurrence in water at diagnostically relevant intensities and pulse durations and an extensive literature demonstrating cavitational effects in plants, fruit flies and *in vitro* systems (NCRP 1983; Nyborg and Ziskin 1985). Yet there is no evidence from research in mammals with diagnostic-like pulse exposures that would suggest a biological effect associated with cavitation in parenchymal tissues without well defined gas bodies (Carstensen and Gates 1984, 1985). Only recently have effects associated with bubbles been reported for lung that contains gas pockets (Child et al. 1990).

The intensity and exposure duration for hind limb paralysis in the neonatal mouse from 1 MHz, continuous wave, unfocused ultrasound at hydrostatic pressures of 0.1 and 1.6 MPa and at 10 and 37°C have been reported previously (Lee and Frizzell 1988). Those results showed that, above a specific intensity level, at each temperature, the exposure duration for paralysis of 50% of specimens exposed (t_{50}) was greater at the increased hydrostatic pressure of 1.6 MPa than at 0.1 MPa. Thus, there was a threshold for cavitational involvement in the paralysis at 0.1 MPa, at each temperature. These thresholds were expressed in terms of the intensity and exposure duration for paralysis of 50% of specimens exposed, *i.e.*, the effective dose 50% (ED_{50}) exposure conditions. The thresholds were reported to fall in the intensity range of 120–150 W/cm^2 and exposure duration range of 1.7–0.92 s at 10°C and to fall in the intensity range of 53–74 W/cm^2 and exposure duration range of 2.8–1.1 s at 37°C. In addition, measurement of the t_{50} at 289 W/cm^2, an intensity above the threshold, and 10°C as a function

[†] Present address: Applied Technology Associates, 1900 Randolph SE, Albuquerque, NM 87106, USA.

[‡] Present address: 2910 Arcade Street, Canada, MN 55109. Address correspondence to: Leon A. Frizzell.

of hydrostatic pressure showed that cavitation was suppressed at hydrostatic pressures above approximately 1 MPa. This result and the threshold for cavitation at 0.1 MPa and 10°C yielded similar values for the threshold negative total pressure associated with the cavitation. Thus, the peak rarefactional pressure P_r was shown to be an important parameter associated with cavitational involvement in hind limb paralysis with continuous wave ultrasound.

Though the results from continuous wave studies have yielded valuable information regarding ultrasound bioeffects, effects produced by short, repetitive pulses are more directly applicable to diagnostic ultrasound. In this study the pulse average intensity and peak rarefactional pressure for hind limb paralysis and lung hemorrhage in the neonatal mouse were determined for pulsed exposure to focused ultrasound. The results show an inverse relation between exposure level, whether pulse average intensity or peak rarefactional pressure, and time.

METHODS

The sonication chamber and most of the electronics were the same as used previously for sonication of neonatal mice (Frizzell et al. 1983; Lee and Frizzell 1988). To generate the high intensities required in these pulsed studies, the transducer was changed from the unfocused quartz source used in the previous studies to a 1 MHz fundamental, lead metaniobate, focused source. The transducer was 7.62 cm (3″) in diameter with a 10.2 cm (4″) radius of curvature. The beam width to 95% of peak intensity was approximately 1 mm, which assures that the intensity incident on the entire spinal cord diameter was within 5% of the spatial peak value. The lossy lead metaniobate material was chosen so that the transducer would be relatively broadband and could be used to produce short pulses of ultrasound.

The electronics for driving the transducer consisted of the following. The 1 MHz output signal from a Wavetek model 3006 synthesized signal generator, with voltage level controlled by an attenuator, was connected to the input of a mixer. The mixer was used as a solid state switch that was turned on by 10 μs rectangular pulses, at the desired pulse repetition frequency (PRF) and exposure duration, provided by an AST Premium 286 personal computer with a Metrabyte DAS-16 analog I/O board. The radio frequency (RF) pulses from the mixer were amplified by a 500-W Electronic Navigation Industries model A-500 wideband amplifier and applied to the transducer. The transducer was calibrated in the linear output range using a thermocouple embedded in an absorbing fluid that was in turn calibrated against a suspended steel ball radiometer. The linearly extrapolated values of the spatial peak, pulse average intensity (I_{SPPA}[lin]) were computed using this calibration.

The specimens were ICR (Hap: (ICR)BR Harlan Industries) Swiss white laboratory mouse neonates harvested within 24 h of birth. The neonates were anesthetized by lowering their body temperature via placement on ice for sonication at 10°C and placed in a specimen holder assembly (see Fig. 1). The head, hind limbs and tail were held by covers within indentations provided in the plexiglass blocks of the holder. The neck was sealed with Vaseline petroleum jelly so that the head and nostrils were dry when the holder was immersed in the degassed Ringer's coupling medium (maintained at 10 ± 0.1°C) within the sonication chamber. The animal breathed through air holes drilled in the plexiglass block, connected to tubes extending above the surface of the coupling medium.

Pressure measurements

After studies had been conducted based on the linear extrapolation of low level calibration results, measurements were made of the field parameters at several intensities using a membrane hydrophone. A polyvinylidene fluoride (PVDF) Marconi Type Y-34-3598 bilaminar shielded membrane hydrophone with an active element 0.5 mm in diameter was used as the

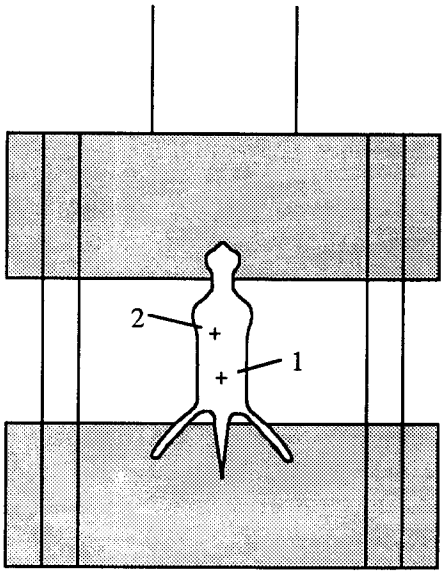

Fig. 1. Drawing of neonate mounted in holder. The head is held in an indentation in one plexiglass bar and the neck is sealed with Vaseline to keep coupling liquid out. The tail and hind limbs are held in another plexiglass bar. The locations labeled 1 and 2 are the sites for sonication of the spinal cord and lungs, respectively.

sensor for field measurements and harmonic assessment. Measurements were made in degassed water at 10°C (density of 1000 kg/m^3 and speed of 1447 m/s). The hydrophone was secured in a circular plexiglass mount and placed at the axial distance from the source corresponding to the position of the mouse during sonication. Measurements were made vs. lateral position, at the fixed axial distance, to position the hydrophone at the spatial maximum.

The hydrophone signal was input to a Tektronix 2430A digital scope and downloaded into an AT&T PC6300 computer for waveform storage and analysis. The spectrum analysis computer program (Zhang 1989) used to run the waveform acquisition and analysis implemented Fast Fourier Transform routines to compute the magnitude of harmonics present in the wave.

The certificate of calibration of the hydrophone from the National Physical Laboratory provided end-of-cable open-circuit sensitivity and impedance for frequencies from 1 to 15 MHz. At 1 MHz, the sensitivity, including the effect of electrical loading, was 0.0346 μV/Pa. This sensitivity value was used to determine the acoustic pressure for calculation of the following parameters, based on the American Institute of Ultrasound in Medicine (AIUM) standard (AIUM, 1992): spatial peak pulse average intensity (I_{SPPA}), pulse duration, pulse intensity integral, maximum compressional pressure (P_c), maximum rarefactional pressure (P_r) and the ratio of second harmonic to the fundamental (P_2/P_1).

Hind limb paralysis

Specimens to be used in the hind limb paralysis study had the dorsal skin overlying the lumbar vertebral region surgically removed. The specimen was mounted in the adjustable holder and aligned using an optical microscope and a high intensity back light so that, upon placing the holder assembly in the sonication chamber, the focal region of the ultrasound beam was centered on the third lumbar vertebral region on the dorsal side of the animal (site 1 in Fig. 1).

The pulse duration and total exposure time were maintained at 10 μs and 2.4 s, respectively, and the PRF and I_{SPPA}[lin] were varied. After sonication the specimen was removed from the sonication chamber and was fully recovered after a 15 min warming period at room temperature. Examination for hind limb paralysis was achieved by gently stimulating the hind feet, tail or belly of the neonate with a small surgical forceps. If no functional alteration had occurred, the animal responded with a strong reflexive movement of the hind limbs. Paralyzed specimens exhibited no reflexive response of the hind limbs.

Approximately 25 mouse neonates were sonicated at a specified intensity and PRF at an exposure duration of 2.4 s (the t_{50} obtained for CW exposures at a linearly extrapolated intensity of 86 W/cm^2) and a temperature of 10°C. This procedure was repeated for five or six different intensities at a common PRF, and the percentage of the specimens with hind limb paralysis was determined at each intensity. Biological variability dictated that there was a range of intensities for which different fractions of specimens, between 0 and 100%, were paralyzed. These results were plotted as the percentage of specimens paralyzed vs. the inverse of the intensity, and a probit analysis (Finney 1971) was performed to determine the intensity for 50% occurrence of paralysis at the specified PRF. This intensity and the exposure duration of 2.4 s specify the effective dose 50% (ED_{50}) for the particular PRF and pulse duration.

Lung hemorrhage

Specimens to be used in the lung hemorrhage study were aligned using an optical microscope so that, upon placing the holder assembly in the sonication chamber, the focal region of the ultrasound beam was incident on the dorsal side of the animal in the region overlying the left lung (site 2 in Fig. 1). After completing the sonication or sham sonication of the specimen, the same experimenter removed the specimen from the chamber, and removed the lungs carefully in a manner designed to minimize trauma to the lungs. The lungs were then delivered to a second person, who did not know whether the lungs were from a sham or sonicated specimen, for examination under a dissecting microscope for evidence of hemorrhage. The lungs from each specimen were scored as hemorrhaged, not hemorrhaged, or uncertain. Those classed as uncertain were not included in the subsequent data analysis. The percentage of animals exhibiting hemorrhage, from the remaining two classifications, was determined for different values of I_{SPPA}[lin]. Even though great care was taken to remove the lungs without causing damage, the lungs are very small and there was a significant percentage of sham sonicated mice exhibiting hemorrhage. Thus, the threshold I_{SPPA}[lin] for hemorrhage was specified as the value where the curve for the percentage of sonicated mice exhibiting hemorrhage intercepted the percentage hemorrhage observed in the shams.

RESULTS

Pressure measurements

The pressure waveforms measured using a membrane hydrophone at I_{SPPA}[lin] = 0.75, 130 and 1800 W/cm^2 are shown in Figs. 2a–c, respectively. It can

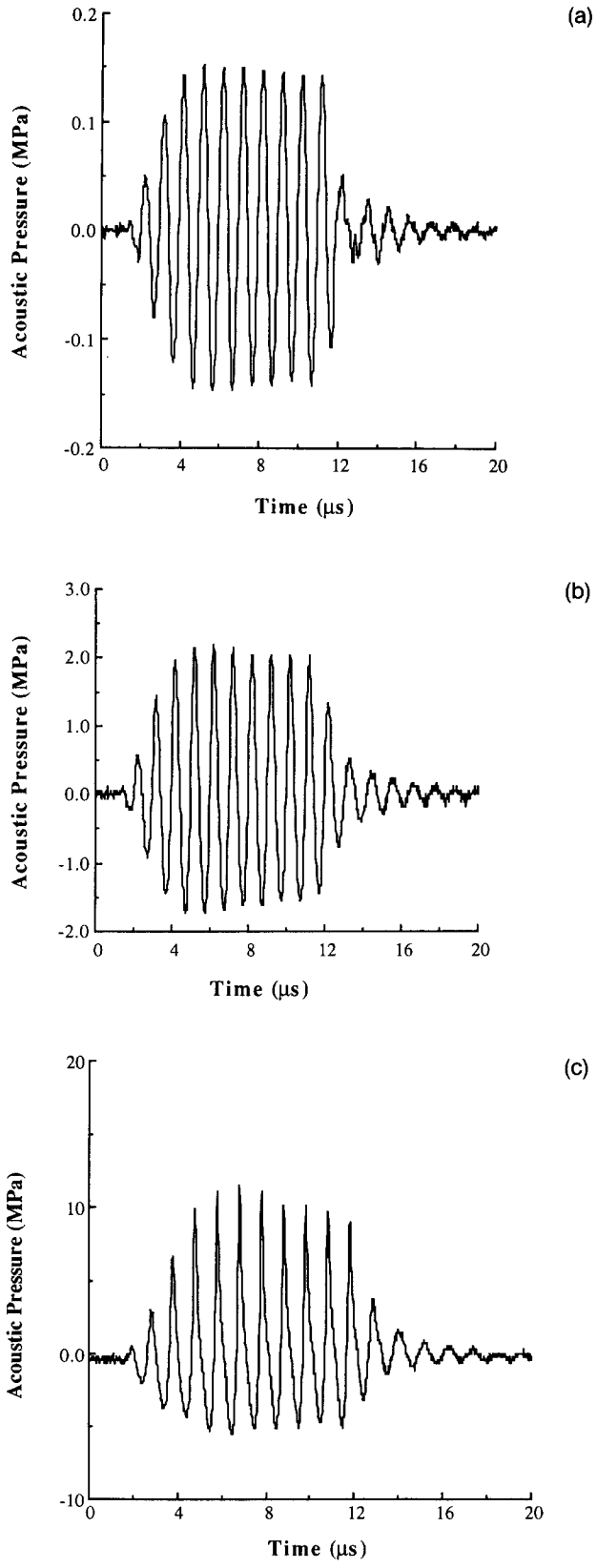

Fig. 2. The pressure waveform as measured using the membrane PVDF hydrophone at I_{SPPA}[lin] values of (a) 0.75 W/cm^2; (b) 130 W/cm^2 and (c) 1800 W/cm^2.

be seen that the pulse increases to full amplitude in about 2–3 cycles and then maintains a relatively constant amplitude until the small amount of ringing that occurs when the excitation is shut off. Except for digitization noise, the waveform at I_{SPPA}[lin] = 0.75 W/cm^2 appears sinusoidal with very little distortion, as expected at this low intensity. Little distortion is evident at 130 W/cm^2, but very significant distortion is apparent at 1800 W/cm^2.

Table 1 lists the spatial peak pulse average intensity (I_{SPPA}), peak compressional pressure (P_c), peak rarefactional pressure (P_r) and P_2/P_1, where P_2 is the amplitude of the second harmonic and P_1 is the amplitude of the fundamental, associated with the intensity levels that were employed for the sonications at PRFs of 5 and 50 kHz. Because of equipment problems, these data are not available for all intensities used in this study.

The hydrophone measurement of I_{SPPA} agreed with I_{SPPA}[lin] at 0.75 W/cm^2 to within 2.5%, showing excellent agreement between the thermocouple calibration and hydrophone measurement methods in the linear range. As the output level increased, the hydrophone measurements of I_{SPPA} decreased relative to I_{SPPA}[lin], the waveform became asymmetric, and the harmonic content increased, as expected due to nonlinear propagation of the wave. This is confirmed by the increased level of the second harmonic relative to the fundamental. It was also determined that the pulse duration averaged approximately 9.1 μs, 9% less than the 10 μs duration of the rectangular pulses applied to the mixer to produce the RF pulses that were applied to the transducer.

Hind limb paralysis

Mouse neonates were sonicated at the third lumbar vertebral region of the spinal cord by 1 MHz, 10 μs pulse duration, repetitively pulsed, focused ultra-

Table 1. Parameters measured by the membrane hydrophone for various values of I_{SPPA}[lin].

I_{SPPA}[lin] (W/cm^2)	I_{SPPA} (W/cm^2)	P_c (MPa)	P_r (MPa)	P_2/P_1 (dB)
0.75	0.731	0.151	0.147	−38
130	118	2.19	1.73	−17
140	111	2.18	1.69	−16.4
150	124	2.3	1.75	−16.2
160	129	2.39	1.77	−15.8
172	141	2.44	1.83	−15.6
800	635	6.75	3.18	−9.6
1000	778	7.88	3.44	−8.8
1200	928	8.79	3.68	−8.4
1400	999	9.58	3.82	−8.0
1600	1080	10.0	4.06	−7.7
1800	1374	12.0	6.0	−8.0

Table 2. ED_{50} exposure conditions for CW and pulsed (10 μs pulse duration and 2.4 s exposure duration) sonication of neonates.

PRF (kHz)	P_H (MPa)	I_{SPPA}[lin] (W/cm^2)	I_{SPPA} (W/cm^2)	P_c (MPa)	P_r (MPa)	On time (s)
CW	0.1	86	65	2.0	1.4	2.4
50	0.1	152	125	2.7	1.8	1.2
50	1.6	229	180	3.5	2.25	1.2
5	0.1	1240	960	9.2	5.1	0.12
5	1.6	1220	940	9.1	5.1	0.12
1	0.1	3000		17.5	7.5	0.024

sound for 2.4 s exposure duration at pulse repetition frequencies of 1, 5 and 50 kHz. At each PRF the value of I_{SPPA}[lin] was determined for paralysis of 50% of the specimens. At PRFs of 5 and 50 kHz, the I_{SPPA}[lin] for paralysis of 50% of the specimens was determined at the increased hydrostatic pressure of 1.6 MPa (16 atmospheres) to suppress any cavitation present. The data are listed in Table 2, including values for I_{SPPA}, P_c, and P_r as determined from interpolation of the data in Table 1.

The data for the ED_{50} exposure conditions at a PRF of 50 kHz show that I_{SPPA}[lin] for paralysis of 50% of the specimens changed from 152 to 229 W/cm^2 (based on Probit analysis of data) when the hydrostatic pressure was increased from 0.1 to 1.6 MPa (see Fig. 3a). This suggests that cavitation was involved in the paralysis at 0.1 MPa.

On the other hand, the data for a PRF of 5 kHz showed a rather different picture (see Fig. 3b). The results at 0.1 MPa hydrostatic pressure showed the percentage paralysis to increase as expected for values of I_{SPPA}[lin] between 800 and 1200 W/cm^2. Up to this point, the results agree with the expected shape of a sigmoidal curve. However, the percentage paralysis leveled off at about 50% at 1200, 1400 and 1600 W/cm^2, and decreased markedly to 15% at 1800 W/cm^2.

One possible explanation for this leveling off and then decrease in percentage paralysis with increasing I_{SPPA}[lin] involves the possibility of cavitation effects in the coupling medium. If, at the higher intensities, the acoustic pressure is high enough to cause cavitation in the coupling medium between the transducer and the mouse, the resultant bubbles can greatly attenuate the sound field, significantly decreasing the ultrasonic energy penetrating the mouse surface. In this manner, the amount of damage, and thus the percentage of animals with hind limb paralysis, would decrease. Observation of surface hemorrhage on the dorsal surface of the mouse occurred in at least 25% of specimens exposed at 1800 W/cm^2, but was not witnessed at the lower intensities. This is indicative of bubbles causing damage at the interface between the Ringer's solution and the mouse.

On the other hand, the percentage paralysis obtained for the 1.6 MPa hydrostatic pressure series, also shown in Fig. 3b, increases monotonically from 15% at 800 W/cm^2 up to 100% at 1800 W/cm^2. A comparison of the percentage paralysis data at 0.1 MPa and at 1.6 MPa hydrostatic pressure shows that the two curves are similar from 800 W/cm^2 up to about 1400 W/cm^2. However, at 1600 and 1800 W/cm^2, the percentage paralysis under conditions of increased hydrostatic pressure is much greater. These results are also consistent with screening by cavitation bubbles in the coupling medium. The pressurization would decrease the amount of cavitation and thus the screening by bubbles at the higher intensities. Thus, it would be expected that more energy reaches the mouse during exposures under increased pressure than during the exposures at atmospheric pressure, resulting in a greater percentage paralysis.

Because the curves at hydrostatic pressures of 0.1 and 1.6 MPa are very similar at the lower intensities, it is likely that *in vivo* cavitation is not involved in causing the hind limb paralysis at a PRF of 5 kHz. Thus, a thermal mechanism appears to be primarily responsible for the paralysis observed. It should also be observed in Fig. 3a that a similar screening phenomenon may have occurred at the higher intensities at 0.1 MPa hydrostatic pressure for the 50 kHz sonications; however, no surface hemorrhage was observed.

Results from exposures at a PRF of 1 kHz are plotted in Fig. 3c. It was not possible to obtain results at the PRF of 1 kHz at the elevated hydrostatic pressure of 1.6 MPa. This was due to a deterioration of the electrical driving system between the time that measurements were completed at 0.1 MPa for all PRFs, and when measurements were attempted at 1 kHz at 1.6 MPa. Thus, no data at increased hydrostatic pressure are available to indicate whether cavitation is involved at this PRF.

Lung hemorrhage

The lungs of mouse neonates were sonicated at 10°C with pulsed ultrasound of 10 μs pulse duration. Specimens were sonicated for 2.4 s at a PRF of 1 kHz, and for 180 s at a PRF of 100 Hz. The percentage of specimens exhibiting hemorrhage versus I_{SPPA}[lin] are listed in Table 3 and graphed in Fig. 4a and b. The data, except for the 700 W/cm^2 datum point at 2.4 s exposure duration, were fit to a second order polynomial using least square analysis. Extrapolation of this fit to the value for percentage hemorrhage observed for the sham sonicated specimens (approximately 32%) gives the threshold values for I_{SPPA}[lin] of 95

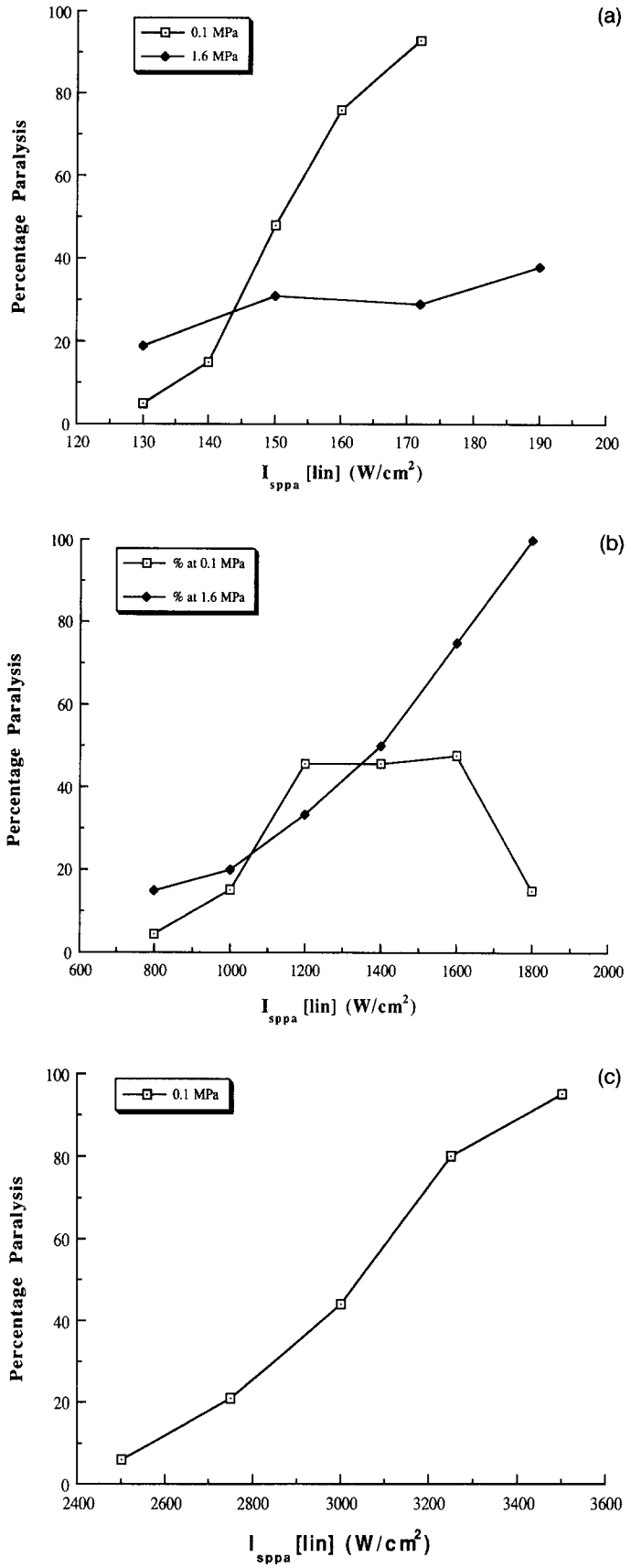

Fig. 3. Percentage of specimens exhibiting hind limb paralysis vs. I_{SPPA}[lin] at 0.1 and 1.6 MPa hydrostatic pressure, 10°C, and 2.4 s exposure duration for 10 μs duration pulses at PRFs of (a) 50 kHz; (b) 5 kHz and (c) 1 kHz.

Table 3. Data for percentage exhibiting hemorrhage in the neonatal mouse lung.

I_{SPPA}[lin] (W/cm^2)	No. showing hemorrhage	No. not showing hemorrhage	Percentage hemorrhaged
For PRF = 1 kHz and exposure duration of 2.4 s			
100	4	8	33
200	6	8	43
300	10	5	67
400	3	0	100
700	5	1	83
For PRF = 100 Hz and exposure duration of 180 s			
10	9	17	35
15	6	5	55
20	6	9	40
25	11	6	65
30	9	9	50
35	12	11	52
50	14	5	74
100	8	2	80

and 4 W/cm^2 for the 2.4 and 180 s exposure durations, respectively. The corresponding values for P_r are 1.5 and 0.37 MPa, respectively, based on an interpolation of data in Table 1.

DISCUSSION

Historically, the levels for biological effects have been compared by examining the spatial peak, temporal average intensity vs. exposure duration as apparent in the old AIUM Statement on Mammalian *In Vivo* Biological Effects (AIUM 1988). It seems appropriate to consider a time averaged quantity for the examination of biological effects associated with a thermal mechanism. However, it has been shown by Carstensen and coworkers (Child et al. 1981) that a quantity associated with the exposure level during a pulse is more appropriate when considering biological effects associated with bubbles or a cavitation phenomenon. Indeed, it may be more revealing to consider a peak quantity such as I_{SPPA} vs. the sound on-time when examining effects of pulsed ultrasound relative to continuous wave ultrasound, even if the dominant mechanism of damage is thermal. This is true primarily because effects associated with low duty cycle pulsed ultrasound will often exhibit nonlinear behavior.

The following argument is presented as a demonstration of the difference between the two presentations of data. Start by assuming that the threshold for several biological effects is directly related to the spatial peak, time average intensity I_{SPTA} and the exposure duration T_{exp} as follows:

$$I_{SPTA} = A\ (T_{exp})^B, \qquad (1)$$

where A and B are constants. For exposures involving linear propagation of pulsed ultrasound with a 10% duty cycle, the I_{SPPA} will be a factor of ten greater than I_{SPTA}, and the sound on-time, T_{on}, will be a factor of ten less than T_{exp}. Substitution into eqn (1) gives the relation

$$I_{SPPA} = A\ 10^{B+1}\ (T_{on})^B, \qquad (2)$$

showing that the power dependence of I_{SPPA} on T_{on} is the same as the power dependence of I_{SPTA} on T_{exp}. For linearly propagating fields, when the duty cycle is known, nothing is lost or gained from this change of parameters. However, now consider that nonlinear propagation becomes increasingly important near the threshold exposures for biological effects from pulsed ultrasound, as for the hind limb paralysis results in this study. A graph of the data from Table 2 obtained at atmospheric pressure in the form I_{SPTA} vs. T_{exp} would show that I_{SPTA} decreases with decreasing PRF at a constant value of T_{exp}. This is expected for a thermal mechanism of damage because the harmonic generation, and thus heating, is greater for the greater peak values associated with lower PRF. Now consider the graph of the same data points in the form I_{SPPA} vs. T_{on} as shown in Fig. 5. This graph allows a more meaningful examination of the role of time. Observation of a deviation from linearity, on a log log plot, indicates clearly the presence of nonlinear effects associated with thermal damage and facilitates a comparison between continuous wave and pulsed results on the same graph. Also, these parameters are more appropriate for examining bubble effects that are related to the level in a pulse as opposed to a time averaged quantity.

Results from the literature and the results from this study are listed in Table 4 and plotted in Fig. 5, in terms of I_{SPPA}[lin] and the sound on time for direct comparison of CW and pulsed data. The data from the literature are representative of effects associated with relatively high level ultrasound exposure, and in most cases involve cavitation in addition to heating. It is important to note here that cavitational effects have been shown to be more directly related to the mechanical index (AIUM/NEMA 1992), which is directly related to P_r divided by the square root of the frequency. Although the value of P_r is provided for the threshold results reported in this study, it is not available for most of the earlier studies, so the quantity used for direct comparison is the linearly extrapolated value of I_{SPPA}. However, a linearly calculated acoustic pressure amplitude (P) scale is also provided in Fig. 5 to give an approximate value for P_r. The pressure amplitude scale was determined by assuming the plane wave relationship

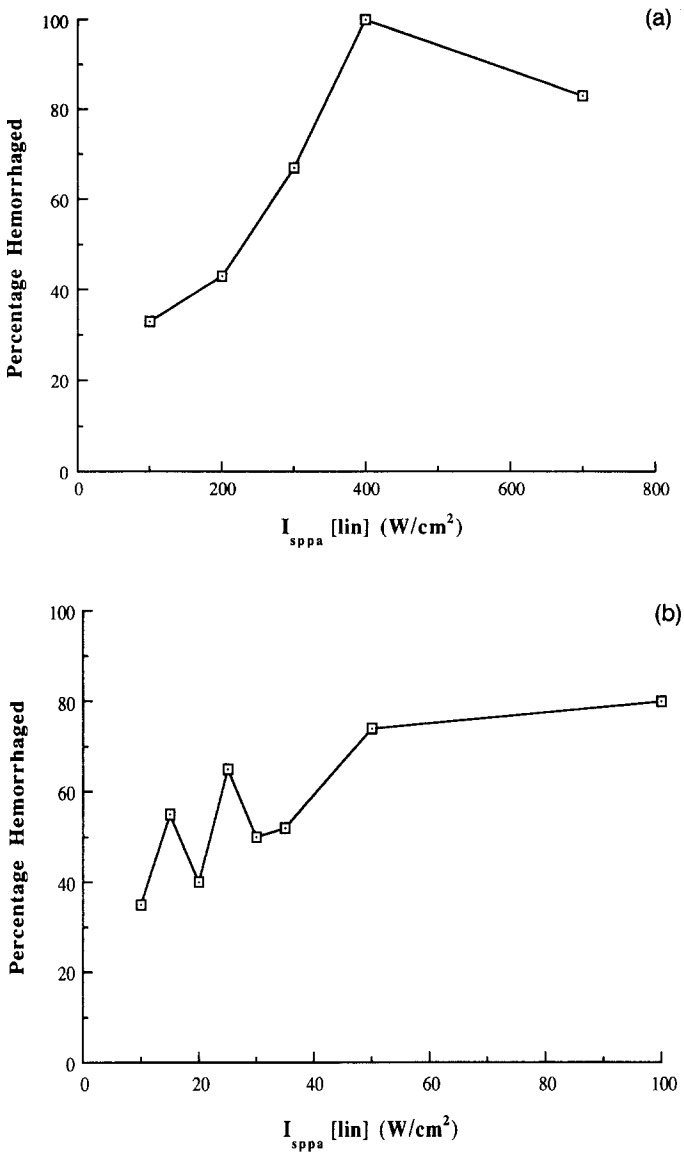

Fig. 4. Percentage of specimens exhibiting lung hemorrhage vs. I_{SPPA}[lin] at 10°C for 10 μs duration pulses at (a) PRF of 1 kHz and exposure duration of 2.4 s and (b) PRF of 100 Hz and exposure duration of 180 s.

$$I = P^2/2\rho c, \quad (3)$$

where I is the pulse average intensity, P is the acoustic pressure amplitude, and a value for the characteristic acoustic impedance $\rho c = 1.62 \times 10^6$ MKS rayls is assumed for tissue at 37°C. The literature results listed in Table 4 and graphed in Fig. 5 are summarized briefly below.

Wong and Watmough (1983) reported hemolysis at 0.75 MHz from exposure to an intensity of approximately 1 W/cm^2, at 5 min sound on time (Result No. 1).

Lehmann and Herrick (1953) demonstrated the formation of petechial hemorrhages at 1 W/cm^2 at 2 min sound on time (Result No. 2). Extensive studies involving increased ambient pressure, temperature changes and frequency changes all suggest cavitation as the responsible mechanism.

Martin et al. (1981) showed lesion formation at the surface of exteriorized mouse liver (Result No. 3). The level at which this occurred was dependent upon the coupling technique but was approximately 2.2 W/cm^2 for 2 min sound on time. The coupling fluid likely supplied the nuclei for cavitation in this case. Thus, this may not strictly be considered an example of cavitation *in vivo*.

Taylor and Pond (1972) reported paralysis in rats at 50 W/cm^2 pulsed exposure for a sound on-time of

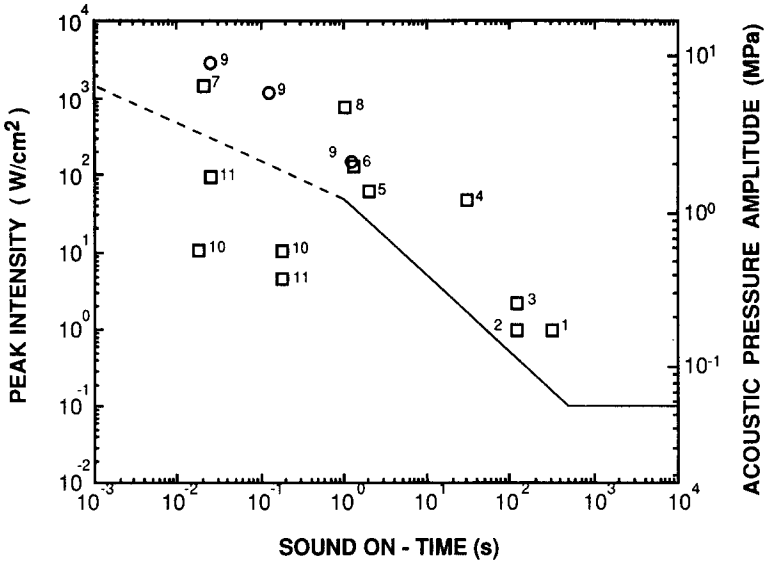

Fig. 5. *In vivo* biological effects plotted as peak intensity and calculated acoustic pressure amplitude versus sound on time.

30 s (5 min exposure duration; Result No. 4). The results of some of their studies with pulsed exposures would suggest that cavitation might be involved. Frizzell and co-workers (Frizzell et al. 1983; Frizzell and Lee 1986; Lee and Frizzell 1988) demonstrated the involvement of cavitation in hind limb paralysis of the neonatal mouse above approximately 53–74 W/cm^2 at 2.8–1.1 s sound on-time at 37°C (Result No. 5) and above the range 120–150 W/cm^2 at 1.7–0.92 s sound on time at 10°C (Result No. 6). Many investigators have reported the threshold for lesion production from focused ultrasound in brain, liver and other tissues (Bassauri and Lele 1962; Fry et al. 1971; Robinson and Lele 1972; Pond 1970; Frizzell et al. 1977; Chan and Frizzell 1977). Recent results from studies of cat liver show the threshold for cavitation involvement to be approximately 1500 W/cm^2 at 20 ms sound on-time (Frizzell 1988) in agreement with that for brain (Result No. 7). Above this intensity, the threshold for cavitation lesions in brain and liver follow an $IT^{1/2} = 200$ W/cm^2 with $s^{1/2}$ dependence.

Hynynen (1991) reported levels for thermally significant cavitation in muscle over the range of frequencies 0.246–1.68 MHz with a value of approximately 800 W/cm^2 for a 1 s exposure (Result No. 8). His results were based on threshold levels for erratic temperature rise as measured with thermocouples.

The results for hind limb paralysis and lung hemorrhage in neonatal mice, as reported in this paper, are listed as numbers 9 and 11, respectively. Carstensen

Table 4. Threshold results from *in vivo* biological effects studies.

Investigators	Effect	Frequency (MHz)	Intensity (W/cm^2)	Sound on time (s)
1. Wong and Watmough	Hemolysis	0.75	1	300
2. Lehmann and Herrick	Petechial Hemorrhages	1	1	120
3. Martin et al.	Lesion formation	0.8	2.2	120
4. Taylor and Pond	Paralysis	0.5–2	50 (P)	30
5. Frizzell et al.	Paralysis (37°C)	1	53	2.8
6. Frizzell et al.	Paralysis (10°C)	1	119	1.7
7. Many	Lesion formation	1–3	1500	0.02
8. Hynynen	Thermally Significant Cav	1	800	1
9. Frizzell et al.	Paralysis (10°C)	1	152 (P)	1.2
			1240 (P)	0.12
			3000 (P)	0.024
10. Child et al.	Lung hemorrhage	1	11 (P)	0.18
			11 (P)	0.018
11. Frizzell	Lung hemorrhage	1	95 (P)	0.024
			4 (P)	0.18

and coworkers (Child et al. 1990) reported that the threshold for lung hemorrhage in adult mouse lung was approximately 11 W/cm^2 for 180 s exposures to 10 μs duration pulses for pulse repetition frequencies of 100 and 10 Hz (Result No. 10).

It is quite clear from Fig. 5 that a graph of I_{SPPA} vs. T_{on} does represent a useful way to compare data from both CW and pulsed studies. Further, it can be seen from Fig. 5 that the hind limb paralysis data from this study show good agreement with similar data from CW studies, and with data for other biological effects associated with tissues that contain no preexisting large gas bodies. However, it is equally clear that the pulse average intensity levels for hemorrhage in lung are well below those for effects in the other tissues that have been examined. In fact, the value of I_{SPPA}[lin] for lung hemorrhage in this study at the 2.4 s exposure duration (0.0024 s sound on-time) and 1 kHz PRF is less than $\frac{1}{30}$ of the value for hind limb paralysis under the same pulsing conditions. Thus, the results from this study using neonatal mice at 10°C provide a direct confirmation of the much lower threshold for effects in lung, as compared to other tissues that do not contain gas bodies, as reported by Carstensen and coworkers (Child et al. 1990) for adult mice.

It is also clear in Fig. 5 that the results for lung hemorrhage obtained in this study show a dependence on sound on-time that is not apparent in the results for adult mouse lung (Child et al. 1990). However, Carstensen and coworkers (Raeman et al. 1993) have recently completed studies that show these results to be consistent. They demonstrated that the exposure duration rather than the sound on-time is the more pertinent parameter for the lung hemorrhage. This shows that an examination of I_{SPPA} vs. sound on-time cannot be uncritically examined without some consideration of exposure duration. In fact, an appropriate examination of the role of time must consider pulse duration, sound on-time and exposure duration.

Finally, the solid lines drawn on Fig. 5 represent a translation of the old AIUM Statement on *In Vivo* Biological Effects (AIUM 1988) to the corresponding levels on a graph of I_{SPPA} vs. T_{on}. The dashed line I_{SPPA}[lin] $(T_{on})^{0.5} = 50$ W s$^{0.5}$ cm^{-2}) represents a possible extension of that statement, based on I_{SPPA} vs. T_{on}, to values of T_{on} less than one second. The combined solid and dashed lines lie below all results except the lung hemorrhage data.

Using these lines and some simple assumptions, it is possible to make some significant statements relative to the likelihood of cavitation damage to tissues, other than those containing well defined populations of stabilized gas bodies as found in lung, from diagnostic ultrasound. Taking a worst case approach, by assuming that the effect of repetitive pulses is cumulative, one can determine the total on-time required to cause a biological effect of the type reported at a specific pulse average intensity or its corresponding pressure amplitude. For example, at a pulse-average, spatial peak intensity of 500 W/cm^2 corresponding to P $\approx$ 4 MPa, the total on-time could be as long as 0.01 s and still not go above the dashed curve of Fig. 5. For a 0.001 duty factor, typical of diagnostic systems, this corresponds to an exposure duration or a dwell time of 10 s. In a typical exam, the dwell time would be less than this because the transducer is being manually, mechanically or electrically scanned. Pulsed Doppler instruments typically have a greater duty factor, so the dwell time would be reduced for a comparable exposure level.

The dashed line in Fig. 5 is shown extending to sound on-time as short as 1 ms. However, it is reasonable to expect that at a sufficiently high intensity, or P_r, just one short, diagnostic-like pulse might be sufficient to cause damage to tissues. Data are not currently available to define that level.

It should also be remembered that the biological effects discussed in this report involve substantial damage to many cells. It is possible that cavitation may occur, producing more subtle damage involving one or a few cells. These effects could occur at lesser exposure conditions. Such effects might not be important to the examination of most organs, but could be important when gonadal tissue or the developing fetus are involved.

Acknowledgements—This study was supported in part by a grant from the National Institutes of Health (CA42369). The authors are indebted to A. Pang, T. Brandenburg, G. Sebesta, K. Pillai and K. James for conducting experiments and helping with some aspects of the data analysis.

REFERENCES

American Institute of Ultrasound in Medicine. Bioeffects considerations for the safety of diagnostic ultrasound. J. Ultrasound Med. 7, No. 9 (supplement); 1988.

American Institute of Ultrasound in Medicine. Acoustic output measurement and labelling standard for diagnostic ultrasound equipment. AIUM, Rockville, MD; 1992.

American Institute of Ultrasound in Medicine/National Electrical Manufacturers Association. Standard for real-time display of thermal and mechanical acoustic output indices on diagnostic ultrasound equipment. AIUM, Rockville, MD; 1992.

Apfel, R. E. Acoustic cavitation: A possible consequence of biomedical uses of ultrasound. Br. J. Cancer. 45:140–146; 1982.

Apfel, R. E. Possibility of microcavitation from diagnostic ultrasound. IEEE Trans. UFFC33:139–142; 1986.

Atchley, A. A.; Frizzell, L. A.; Apfel, R. E.; Holland, C.; Madenshetty, S.; Roy, R. Thresholds for cavitation produced in water by pulsed ultrasound. Ultrasonics 26:280–285; 1988.

Basauri, L.; Lele, P. P. A simple method for production of trackless focal lesions with focused ultrasound: Statistical evaluation of the effects of irradiation on the central nervous system of the cat. J. Physiol. 160:513–534; 1962.

Carstensen, E. L.; Flynn, H. G. The potential for transient cavitation with microsecond pulses of ultrasound. Ultrasound Med. Biol. 8:L720–L724; 1982.

Carstensen, E. L.; Gates, A. H. The effects of pulsed ultrasound on the fetus. J. Ultrasound Med. 3:145–147; 1984.

Carstensen, E. L.; Gates, A. H. Ultrasound and the fetus. In: Nyborg, W. L.; Ziskin, M. C., eds. Biological effects of ultrasound. New York: Churchill Livingstone; 1985:85–95.

Chan, S. K.; Frizzell, L. A. Ultrasonic thresholds for structural changes in the mammalian liver. 1977 Ultrasonic Symposium Proceedings IEEE Cat. #77CH1264-1SU; 1977:153–156.

Child, S. Z.; Carstensen, E. L.; Lam, S. K. Effects of ultrasound on *drosophila:* III. Exposure of larvae to low-temporal-average-intensity, pulsed irradiation. Ultrasound Med. Biol. 7:167–173; 1981.

Child, S. Z.; Hartman, C. L.; Schery, L. A.; Carstensen, E. L. Lung damage from exposure to pulsed ultrasound. Ultrasound Med. Biol. 16:817–825; 1990.

Crum, L. A.; Fowlkes, J. B. Acoustic cavitation generated by microsecond pulses of ultrasound. Nature 319:52–54; 1986.

Finney, D. J. Probit analysis. London: Cambridge University Press; 1971.

Flynn, H. G. Generation of transient cavities in liquids by microsecond pulses of ultrasound. J. Acoust. Soc. Am. 72:1926–1932; 1982.

Fowlkes, J. B.; Crum, L. A. Cavitation threshold measurements for microsecond length pulses of ultrasound. J. Acoust. Soc. Am. 83:2190–2201; 1988.

Frizzell, L. A. Threshold dosages for damage to mammalian liver by high intensity focused ultrasound. IEEE Trans. Ultrason. Ferroelec. Freq. Control. 35:578–581; 1988.

Frizzell, L. A.; Lee, C. S. Exposure levels for ultrasonic cavitation in mammals. Proceedings of the Eighth Annual Conference, IEEE Eng. Med. Biol. Soc., Fort Worth, Nov. 7–10; 1986:1026–1028.

Frizzell, L. A.; Lee, C. S.; Aschenbach, P. D.; Borrelli, M. J.; Morimoto, R. S.; Dunn, F. Involvement of ultrasonically induced cavitation in the production of hind limb paralysis of the mouse neonate. J. Acoust. Soc. Am. 74:1062–1065; 1983.

Frizzell, L. A.; Linke, C. A.; Carstensen, E. L.; Fridd, C. W. Thresholds for focal ultrasonic lesions in rabbit kidney, liver, and testicle. IEEE Trans. Biomed. Eng. BME-24:393–396; 1977.

Fry, F. J.; Kossoff, G.; Eggleton, R. C.; Dunn, F. Threshold ultrasound dosages for structural changes in mammalian brain. J. Acoust. Soc. Am. 48:1413–1417; 1971.

Holland, C. K.; Apfel, R. E. An improved theory for the prediction of microcavitation due to pulsed ultrasound. IEEE Trans. UFFC 36:204–208; 1989.

Hynynen, K. The threshold for thermally significant cavitation in dog's thigh muscle *in vivo.* Ultrasound Med. Biol. 17:157–169; 1991.

Lee, C. S.; Frizzell, L. A. Exposure levels for ultrasonic cavitation in the mouse neonate. Ultrasound Med. Biol. 14:735–742; 1988.

Lehmann, J. F.; Herrick, J. F. Biologic reactions to cavitation, a consideration for ultrasonic therapy. Arch. Phys. Med. 34:86–98; 1953.

Martin, C. J.; Gregory, D. W.; Hodgkiss, M. The effects of ultrasound in vivo on mouse liver in contact with an aqueous coupling medium. Ultrasound Med. Biol. 7:253–265; 1981.

National Council on Radiation Protection and Measurements. Biological effects of ultrasound: Mechanisms and clinical implications. NCRP: Bethesda, MD, Report no. 74; 1983.

Nyborg, W. L.; Ziskin, M. C., eds. Biological effects of ultrasound. New York: Churchill Livingstone; 1985.

Pond, J. B. The role of heat in the production of ultrasonic focal lesions. J. Acoust. Soc. Am. 47:1607–1611; 1970.

Raeman, C. H.; Child, S. Z.; Carstensen, E. L. Timing of exposures in ultrasonic hemorrhage of murine lung. Ultrasound Med. Biol. 19:507–512; 1993.

Robinson, T. C.; Lele, P. P. An analysis of lesion development in the brain and in plastics by high-intensity focused ultrasound at low-megahertz frequencies. J. Acoust. Soc. Am. 51:1333–1351; 1972.

Taylor, K. J. W.; Pond, J. B. A study of the production of haemorrhagic injury and paraplegia in rat spinal cord by pulsed ultrasound of low megahertz frequencies in the context of the safety for clinical usage. Brit. J. Radiol. 45:343–353; 1972.

Wong, Y. S.; Watmough, D. J. Haemolysis of red blood cells in vitro and in vivo induced by ultrasound at 0.75 MHz and at therapeutic intensity levels. In: Miller, R.; Rosenfeld, R.; Cobet, U., eds. Ultrasound interaction in biology and medicine. New York: Plenum Press; 1983:179–184.

Zhang, J. Influences of structural factors of biological media on the acoustic nonlinearity parameter B/A. Ph.D. Dissertation, University of Illinois, Urbana-Champaign; 1989.